

# PRINCIPLE AND APPLICATIONS OF MICROBUBBLE FLOODING TECHNOLOGY FOR ENHANCED OIL RECOVERY

---

### Li Yisong

Research Institute of Petroleum  
Exploration and Development, China  
National Petroleum Corporation  
RIPED,CNPC

### Lyu Weifeng

Research Institute of Petroleum  
Exploration and Development, China  
National Petroleum Corporation  
RIPED,CNPC

### Zhang Qun

Research Institute of Petroleum  
Exploration and Development, China  
National Petroleum Corporation  
RIPED,CNPC

### Ding Bin

Research Institute of Petroleum  
Exploration and Development, China  
National Petroleum Corporation  
RIPED,CNPC

### Wu Jiazhong

Research Institute of Petroleum  
Exploration and Development, China  
National Petroleum Corporation  
RIPED,CNPC

### Chen Xinglong

Research Institute of Petroleum  
Exploration and Development, China  
National Petroleum Corporation  
RIPED,CNPC

### Li Ying

Research Institute of Petroleum  
Exploration and Development, China  
National Petroleum Corporation  
RIPED,CNPC

### Guan Modi

Research Institute of Petroleum  
Exploration and Development, China  
National Petroleum Corporation  
RIPED,CNPC

**ABSTRACT:** Microbubble flooding technology has proven significant potential for enhancing oil recovery in low permeability reservoirs. In the pilot test of Changqing Oilfield (16 injection wells and 68 production wells), microbubble flooding led to a 2.8% increase in the dynamic recovery factor over 4 years. The cumulative incremental oil production reached 17,085 tons, with a net increase of 7,225 tons, accounting for 43.6% of total production. The oil recovery improved by 14.6% compared to conventional water flooding. Microbubble flooding technology is able to enhance fluid mobility, reduce oil viscosity, and increase sweep efficiency, effectively displacing the residual oil droplet trapped in smaller pores.

throats. The pilot test demonstrated substantial economic benefits, with an internal rate of return (IRR) of 14.94% and a net present value (NPV) of 10.42 million USD. These results highlight the long-term effectiveness and sustainability of microbubble flooding for enhancing oil recovery in low permeability reservoirs.

**KEYWORDS:** Enhanced oil recovery (EOR), Low permeability reservoir, Microbubbles, Bubble generation, Mechanisms

## INTRODUCTION

In recent years, many oilfields in China (particularly those with low permeability reservoirs) have reached high or extra-high water-cut stages. The strong heterogeneity, fractures, and significant permeability differences lead to complex micro pore-throat network distributions and oil-water seepage mechanisms (Fang et al., 2019). Traditional water and gas flooding in low permeability reservoirs frequently face limitations such as poor sweep efficiency, difficulty in penetrating low-permeability zones, formation energy loss, and the tendency for injected fluids to preferentially flow through high-permeability channels (Ding et al., 2022). These issues lead to uneven oil displacement and ineffective flooding cycles, which result in low oil recovery rates. Therefore, it is crucial to develop a new technology to improve the displacement profiles and block the large pore throat, thereby expanding the sweep efficiency and increasing the oil recovery.

Microbubble flooding technology has emerged as a promising method for enhanced oil recovery (EOR), offering significant potential in improving sweep efficiency and mobilizing residual oil in a variety of reservoir conditions. It operates without the need for chemical agents, making it a cost-effective and environmentally friendly solution. In Changqing Oilfield (16 injection wells and 68 production wells), it delivered a remarkable result as a 2.8% increase in dynamic recovery factor over four years compared to conventional water flooding.

Microbubbles, defined as gas bubbles with diameters ranging from 50 to 250 micrometers, exhibit unique properties such as increased surface area, high gas retention capacity, and the ability to generate local pressure gradients within porous media (Agarwal et al., 2011). These characteristics enable microbubbles to enhance fluid flow and significantly alter the dynamics of oil displacement, particularly in challenging reservoirs with low permeability and high oil viscosity. The principle of microbubble flooding revolves around the injection of microbubbles into the reservoir, where they interact with the reservoir fluids, promoting oil displacement through a combination of mechanisms (Li et al., 2024). These include the reduction of residual oil saturation, increased emulsification of crude oil, and the improvement of fluid mobility. The presence of microbubbles within the reservoir significantly alters the flow behavior by inducing pressure fluctuations, creating a dynamic interface between the oil and water phases, which facilitates more efficient oil displacement. Furthermore, microbubbles serve to lower the viscosity of the oil phase, increase the injectivity of fluids, and improve the overall sweep efficiency during flooding operations (Q. Liu et al., 2024). This paper introduces the microfluidic experiments and application status in low permeability reservoirs.

## MATERIALS AND METHODS

### Materials

The experimental setup consists of several key components: 1) a Quizix 5210 displacement pump, which precisely controls the injection rate with an accuracy of 0.0001 mL/min, ensuring precise fluid management within the model's pores; 2) ZEISS V8 stereomicroscope provides magnification of images within the pores, with a maximum objective magnification of 16x under wide-field conditions; 3) FASTCAM Mini high-speed camera captures dynamic flow patterns within micron-scale pores, operating at a collection frequency of 8,000 fps and a resolution of 1,024×1,024 pixels; 4) the effective area of visualization microfluidic model is 40 mm × 40 mm, with pore throats ranging from 80 to 300  $\mu\text{m}$ , withstanding temperatures up to 120°C and pressures up to 20 MPa; 5) deionized (DI) water at room temperature ( $24 \pm 1^\circ\text{C}$ ), with a conductivity of 1.5  $\mu\text{S}/\text{cm}$  and pH of 6.5, was used to prepare the aqueous dispersions of microbubbles; 6) methylene blue, sourced from SigmaÒ (St. Louis, MO, USA), was utilized as a contrast agent for microbubble fluid; 7) oil sample is aviation kerosene, with a viscosity of 1.25 mPa·s at 25°C and atmospheric pressure; 8) gas medium is CO<sub>2</sub>, with a purity of 99.99%; 9) the gas source of microbubble generation is CO<sub>2</sub> and the microbubbles were generated by orifice plate method, with bubble diameters of  $(35 \pm 10) \mu\text{m}$  as Figure 2 and Figure 3; 10) liquid to gas ratio is 3:1.

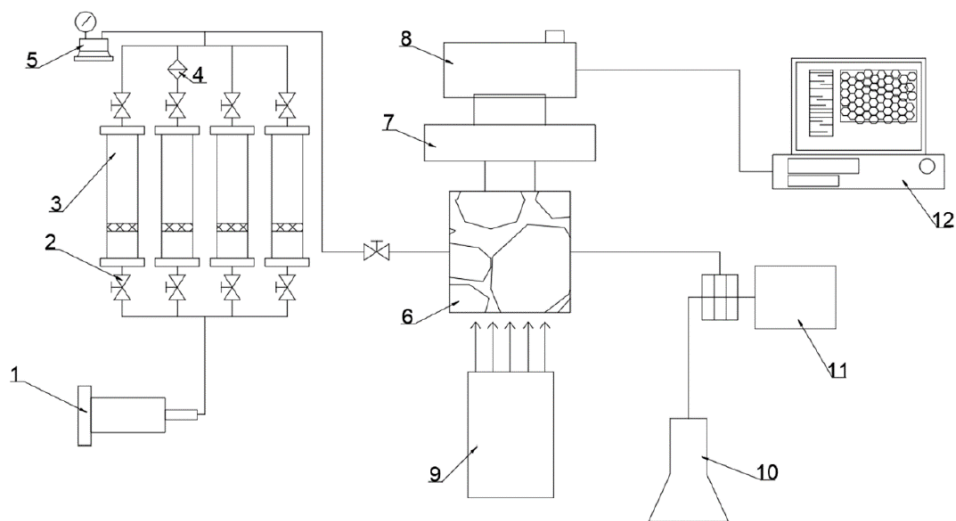


Figure 1 – Microfluidic visual oil displacement experimental setup

1. Displacement pump; 2. Switch valve; 3. Intermediate container (from left to right: oil, water, CO<sub>2</sub>, microbubble fluid); 4. Filter; 5. Pressure gauge; 6. Microfluidic etched glass model; 7. ZEISS microscope; 8. High-speed camera; 9. Light source; 10. Conical flask; 11. Backpressure valve; 12. Computer

Source: produced by the author



2) Vacuum and saturation of the etched model: apply a vacuum to the microfluidic model and saturate it with water. Connect the vacuum device and verify the sealing integrity. Start the vacuum pump, and once the vacuum pressure stabilizes at 0.1 MPa for one hour, proceed with water saturation. After continuing the evacuation for an additional 10 minutes, turn off the pump and valve, then begin video recording to document the water saturation status of the etched glass model.

3) Oil saturation and bound water creation: perform oil saturation and bound water formation through flooding. Ensure that no water exits the model's pores and that the model becomes filled with the oil sample. Simultaneously, collect at least 1 mL of oil in the collection bottle. Image data will be intermittently captured during the flooding process, and the final results will be recorded.

4) Water flooding: carry out water flooding at a constant flow rate, capturing images throughout the entire process to monitor the progression of the flooding.

5) CO<sub>2</sub> miscible flooding and microbubble flooding: similarly, perform CO<sub>2</sub> immiscible flooding and microbubble flooding. Repeat steps 3 and 4 for each method. The flooding speed and operational parameters for each technique are detailed in Table 1.

6) Experimental analysis: visual observation and analysis of the captured images. Image processing software, ImagePro Plus 6.0, is used to identify and classify the oil, water, and gas phases in the model.

Operation name	Oil saturation	Water flooding	Gas flooding	Microbubble flooding
Flooding speed (mL·min <sup>-1</sup> )	0.03	0.1	0.1	0.1
High speed camera frequency (fps)	400	400	800	1800

Table 1 – Flooding speed and operational parameters

Source: produced by the author

## RESULTS AND DISCUSSION

### Microfluidic visual oil displacement experimental

Water flooding is conducted after the oil saturation process. As shown in Figure 4, the water displaces oil in the affected pore throats in a piston-like manner during the water flooding process, which effectively displaces oil from the smaller pores. However, in larger pores, only a portion of the oil is displaced, leaving a significant amount of columnar residual oil in the smaller pore throats. In contrast, during CO<sub>2</sub> immiscible flooding, the CO<sub>2</sub> displaces oil in a non-piston-like manner along the center of the pores and throats, resulting in a higher residual oil accumulation in a membrane-like form along the pore walls. According to Table 2, the comparison between water flooding and CO<sub>2</sub> immiscible flooding shows that the oil recovery from water flooding reaches 79.2%, and CO<sub>2</sub> immiscible flooding

improves the recovery by an additional 9.2% compared to water flooding (reached 88.4%). Specifically, CO<sub>2</sub> immiscible flooding can lower interfacial tension, reduce oil viscosity, improve displacement efficiency, and increase pressure to mobilize trapped oil (Fang et al., 2019). These combined mechanisms make CO<sub>2</sub> flooding more effective, especially in reservoirs with high residual oil saturation conditions.

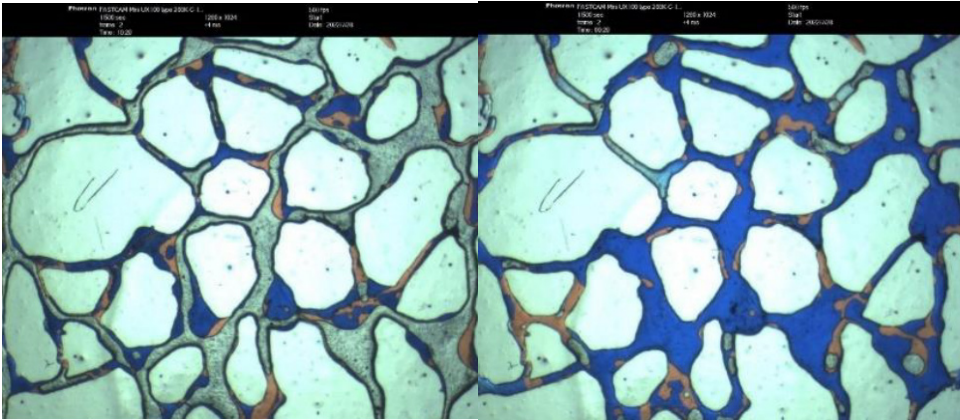


Figure 4 – Comparison between water flooding and CO<sub>2</sub> immiscible flooding (left: water flooding; right: CO<sub>2</sub> immiscible flooding)

Source: produced by the author

	Oil phase area/pixel points	Oil recovery (%)
End of oil saturation	231821	-
End of waterflooding	43950	79.20%
End of CO <sub>2</sub> immiscible flooding	26115	88.40%

Table 2: The results of water flooding and CO<sub>2</sub> immiscible flooding

Source: produced by the author

As mentioned above, CO<sub>2</sub> was the gas medium to generate microbubble. As shown in Table 3, upon a comparison between water flooding and microbubble flooding, the recovery from water flooding reaches 81.5% while microbubble flooding enhances the recovery by 14.6%.

	Oil phase area/pixel points	Oil recovery (%)
End of oil saturation	228029	-
End of waterflooding	39460	81.50%
End of CO <sub>2</sub> immiscible flooding	10582	96.10 %

Table 3: The results of water flooding and microbubble flooding

Source: produced by the author

During water flooding, water displaces oil in a piston-like manner (Al-Saedi et al., 2020). However, the oil becomes “water-locked” in smaller pore throats once the dominant flow channels are formed, which is one of the primary reasons for the low efficiency of water flooding. In contrast, microbubble flooding leverages the merging of small bubbles to form larger bubbles, as shown in Figure 5. These larger bubbles temporarily block the flow channels, increasing flow resistance and causing the subsequent displacing fluids to redirect toward smaller pore throats (N. Liu et al., 2021; Telmadarreie et al., 2016). This process displaces the residual oil trapped in the un-swept areas, ultimately improving oil recovery efficiency.

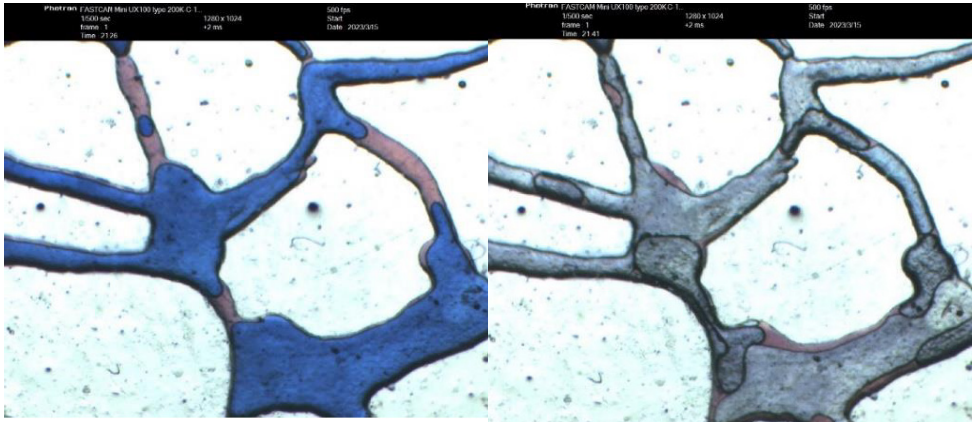


Figure 5: Comparison between water flooding and microbubble flooding (left: water flooding; right: microbubble flooding)

Source: produced by the author

Specifically, the microbubble fluid flows along the path initially created by water flooding. During the displacement process, the microbubbles merge to form larger bubbles, as shown in Figure 6 - Images 1 and 2. When these larger bubbles form, they temporarily block the pores. During the subsequent flow process, the bubbles deform, as depicted in Figure 6 - Images 3 and 4. The deformation of the bubbles, along with the capillary effect and the temporary “blocking” action in the pores, increases flow resistance in the dominant flow channels established by water flooding (Zhang et al., 2024). As a result, the displacing fluids redirect into smaller pores, helping to mobilize and displace the columnar residual oil, thereby expanding the swept volume (Telmadarreie et al., 2016).



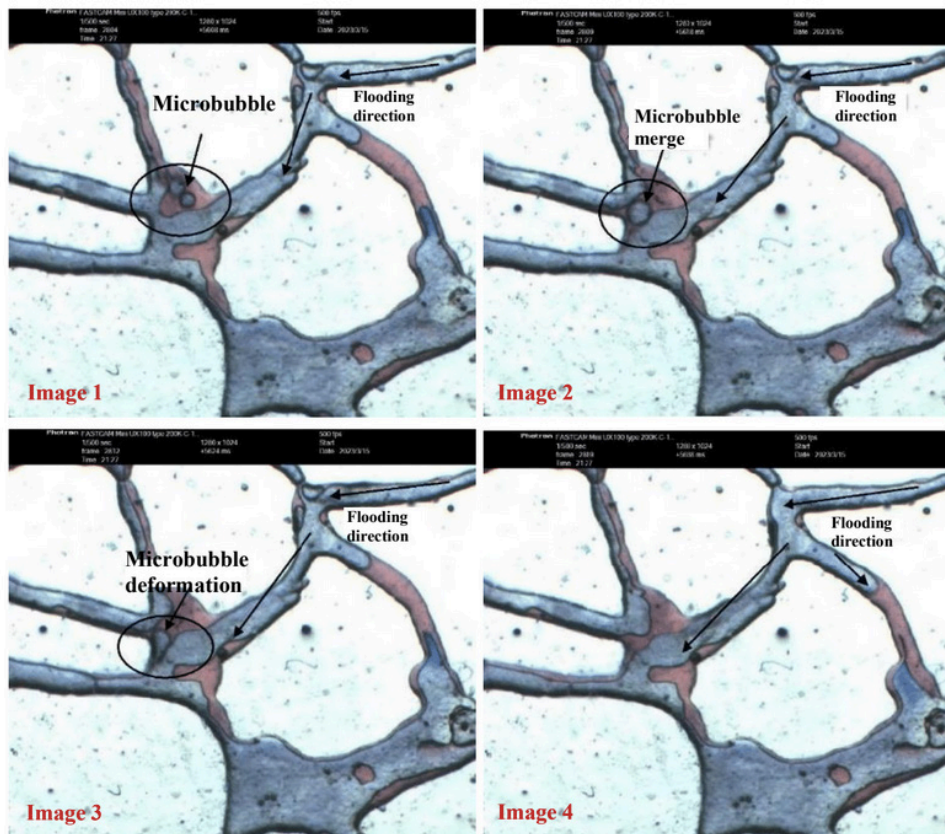


Figure 6: Microbubble oil displacement process

Source: produced by the author

## Oilfield application

The microbubble flooding technology implemented in the Changqing oilfield pilot test area has been operational for 52 months. The pilot project in Wuliwan Block 1, which involves 16 injection wells and 68 production wells, represents the first large-scale demonstration of this technology. Since its inception in 2020, the dynamic recovery factor has increased by 2.8%, achieving an output-to-input ratio of 1.54, indicating the significant effectiveness of the method. To date, the cumulative incremental oil production has reached 17,085 tons, with a net oil increase of 7,225 tons, accounting for 43.6% of the total production. The internal rate of return (IRR) stands at 14.94%, and the financial net present value (NPV) is 10.42 million US\$.

The pilot test was carried out in two phases: Phase I (Figure 7), which began in October 2020 with 4 injection wells, produced 11,063 tons of incremental oil, including a net increase of 5,554 tons. During this phase, the natural decline rate decreased by 17.6%



to 4.5%, and the water cut rate decreased by 2.3% to 2.1%. Phase II (Figure 8), initiated in December 2022 with 12 injection wells, resulted in 6,022 tons of incremental oil, including a net increase of 1,725 tons. During this phase, the natural decline rate decreased by 14.2% to 1.9%, and the water cut rate dropped by 9.9% to 1%. Over 3.7 years, the dynamic recovery factor has risen by 2.8%, demonstrating the technology's long-term effectiveness and substantial contribution to enhanced oil recovery in the region.

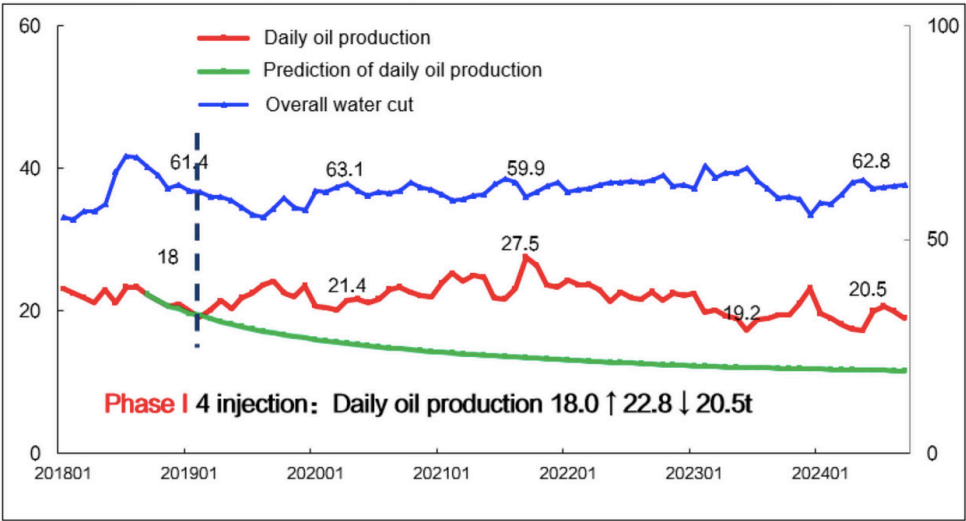


Figure 7: Phase I pilot well group production curve  
Source: produced by the author

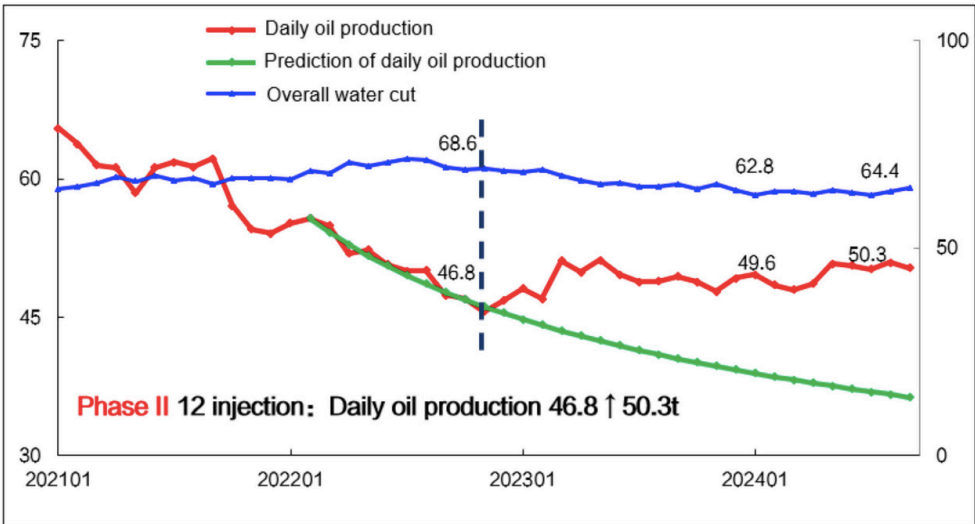


Figure 8: Phase II pilot well group production curve  
Source: produced by the author

## CONCLUSION

In conclusion, microbubble flooding technology represents a promising approach for enhancing oil recovery, particularly in low permeability reservoirs where conventional methods have limited success. The technology's ability to reduce capillary pressure and significantly improve sweep efficiency. Laboratory experiments and field case studies have demonstrated the potential of microbubbles to improve recovery rates, particularly in reservoirs with low permeability or high water cut. However, challenges such as bubble stability, reservoir heterogeneity, and cost-effectiveness must be add. Further research is needed to optimize the generation of microbubbles, improve their stability, and refine injection strategies to maximize recovery. Additionally, numerical simulations will continue to play a critical role in predicting and optimizing the performance of microbubble flooding in a variety of reservoir conditions.

## REFERENCES

- 1) Agarwal, A., Ng, W. J., & Liu, Y. (2011). Principle and applications of microbubble and nanobubble technology for water treatment. *Chemosphere*, 84(9), 1175–1180. <https://doi.org/10.1016/j.chemosphere.2011.05.054>
- 2) Al-Saedi, H. N., Qubian, A., Al-Bazzaz, W., & Flori, R. (2020, January 13). *Experimental Study of Low Salinity Water Flooding: The Effect of Polar Organic Components in Low-Permeable Sandstone Reservoir*. International Petroleum Technology Conference. <https://doi.org/10.2523/IPTC-19740-MS>
- 3) Ding, M.-C., Li, Q., Yuan, Y.-J., Wang, Y.-F., Zhao, N., & Han, Y.-G. (2022). Permeability and heterogeneity adaptability of surfactant-alternating-gas foam for recovering oil from low-permeability reservoirs. *Petroleum Science*, 19(3), 1185–1197. <https://doi.org/10.1016/j.petsci.2021.12.018>
- 4) Fang, T., Wang, M., Gao, Y., Zhang, Y., Yan, Y., & Zhang, J. (2019). Enhanced oil recovery with CO<sub>2</sub>/N<sub>2</sub> slug in low permeability reservoir: Molecular dynamics simulation. *Chemical Engineering Science*, 197, 204–211. <https://doi.org/10.1016/j.ces.2018.12.016>
- 5) Li, S., Wang, X., Wang, S., Zhang, Y., Chen, C., Jiang, L., Wang, L., Liang, F., Sun, H., & Song, Y. (2024). Optimizing oil recovery with CO<sub>2</sub> microbubbles: A study of gas composition. *Energy*, 302, 131836. <https://doi.org/10.1016/j.energy.2024.131836>
- 6) Liu, N., Chen, X., Ju, B., He, Y., Yang, Y., Brantson, E. T., & Tian, Y. (2021). Microbubbles generation by an orifice spraying method in a water-gas dispersion flooding system for enhanced oil recovery. *Journal of Petroleum Science and Engineering*, 198, 108196. <https://doi.org/10.1016/j.petrol.2020.108196>
- 7) Liu, Q., Liu, S., Li, Y., Liu, Y., Wang, N., Yang, Q., & Lu, H. (2024). Microbubble-based process for the enhancement of microfine and heavy oil droplets swirl separation in axial inlet hydrocyclone. *Separation and Purification Technology*, 332, 125642. <https://doi.org/10.1016/j.seppur.2023.125642>
- 8) Telmadarreie, A., Doda, A., Trivedi, J. J., Kuru, E., & Choi, P. (2016). CO<sub>2</sub> microbubbles – A potential fluid for enhanced oil recovery: Bulk and porous media studies. *Journal of Petroleum Science and Engineering*, 138, 160–173. <https://doi.org/10.1016/j.petrol.2015.10.035>
- 9) Zhang, M., Chen, X., Lyu, W., & Han, H. (2024). Mechanisms of microbubble vibration in water-gas dispersion system enhancing microscopic oil displacement efficiency. *Petroleum Exploration and Development*, 51